

# A 3D Analytic Homogenization Model for the Orthotropic Plates with the Type of Double Corrugated Cardboard

Pham Tuong Minh Duong  
Thai Nguyen University of Technology, Vietnam

**ABSTRACT:** In this paper, a 3D complete analytic homogenization model for the corrugated cardboard plates and its application to the crushing and bending modeling of corrugated cardboards are presented. This homogenization model is carried out in two steps. In the first step, we determine the global rigidities of an equivalent homogeneous plate. In the second step, we transform the homogenized plate into an orthotropic solid composed of several layers and we identify the material parameters to take into account for the elasto-plastic behavior through the thickness of the plate. This 3D complete homogenization model can be used not only for corrugated cardboard plates, but also for naval and aeronautic composite structures.

**Keywords:** Analytical homogenization, corrugated cardboard, orthotropic plates.

## I. INTRODUCTION

In the packaging industry, corrugated cardboard plates (cartons) are used widely. It is essential to predict the mechanical behavior of such materials. The numerical modeling of this kind of orthotropic composite plates by shell elements is too tedious and time consuming. Many homogenization models were obtained by analytical, numerical and experimental methods [1-10]. By using some FE models and commercial FE software, the mechanical behaviors of corrugated cardboard were studied by other authors [11-12]. Many studies on the problems of tension, bending and shear, few studies on the problems of torsion, but work on the crushing problems are rare or nonexistent in the literature.

The corrugated cardboard is produced by a converting process in which three or more layers are laminated together. The flat layers are called liners and the corrugated cores are referred to as flutes (Fig. 1). Corrugated cardboard is one of the most used packaging materials to make boxes or interlayers for goods transport. The manufacturing process gives three characteristic directions: the machine direction (MD), the cross direction (CD), and the thickness direction (ZD).

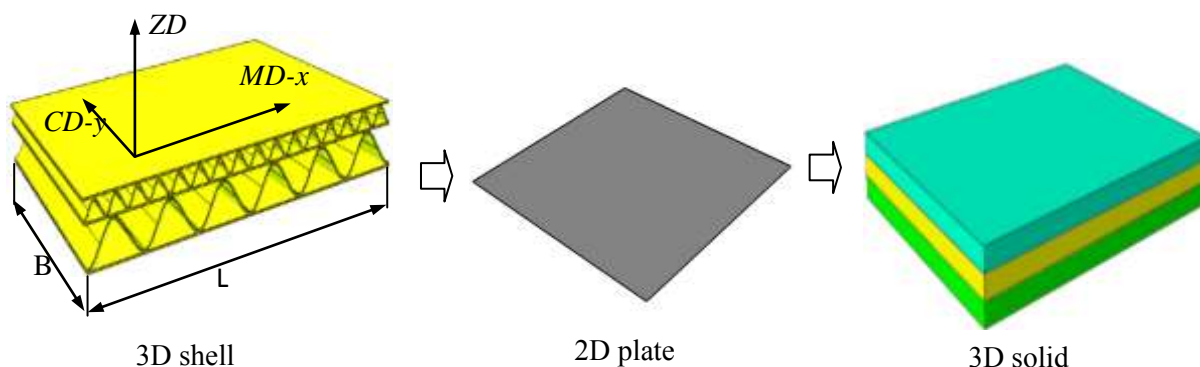


Fig. 1 Two stages of homogenization

This paper presents an efficient homogenization model for the mechanical behavior of a corrugated cardboard composed of three or five layers (single or double flute). Since the flute varies continuously through the thickness, it is difficult to transform this 3D shell structure into a 3D solid immediately. So we propose to carry out the homogenization in two stages (Fig. 1): 1) the global rigidities of the corrugated cardboard are analytically calculated and this 3D structure is replaced by an equivalent homogenized 2D plate; 2) to take into

account the elasto-plastic behavior through the thickness, we retransform the 2D plate into an orthotropic solid composed of several layers and identify the material parameters by using the previous global rigidities. The elasto-plastic simulations and experimental tests on the crushing and bending of a round corrugated cardboard plate by system of mortar-pestle will be studied in this article. This 3D solid homogenization model (implemented into Abaqus software) is quite fast but gives very close results compared to the 3D modeling using the Abaqus shell elements and experimental results.

## II. HOMOGENIZED MODEL FOR CORRUGATED CARDBOARD

A 3D geometrical modeling of the liners and the flutes of the corrugated cardboard is a very tedious and time-consuming task. In our homogenization model, a corrugated cardboard panel is replaced by a 2D plate. Instead of using a local constitutive law (relating the strains to the stresses) at each material point, the homogenization leads to global rigidities (relating the generalized strains to the resultant forces) for the equivalent homogeneous plate.

According to the theory of laminated plates, and by integrating the stresses through the thickness ( $z$ ) and then along the MD direction ( $x$ ), we obtain the following generalized constitutive law [5]:

$$\begin{bmatrix} \{N\} \\ \{M\} \\ \{T\} \end{bmatrix} = \begin{bmatrix} [A] & [B] & [0] \\ [B] & [D] & [0] \\ [0] & [0] & [F] \end{bmatrix} \begin{bmatrix} \{\varepsilon_m\} \\ \{\kappa\} \\ \{\gamma_s\} \end{bmatrix} \quad (1)$$

where  $\{N\}$ ,  $\{T\}$  and  $\{M\}$  are the internal forces and moments;  $[A]$ ,  $[D]$ ,  $[B]$  and  $[F]$  are the stiffness matrices related to the membrane forces, the bending-torsion moments, the bending-torsion-membrane coupling effects and the transverse shear forces respectively;  $\{\varepsilon_m\}$  is the membrane strain vector,  $\{\kappa\}$  is the curvature vector and  $\{\gamma_s\}$  is the transverse shear strain vector. The terms of the stiffness matrices can be calculated as follow:

$$\begin{aligned} A_{ij} &= \sum_{k=1}^n [h^k - h^{k-1}] Q_{ij}^k = \sum_{k=1}^n Q_{ij}^k t^k \\ B_{ij} &= \frac{1}{2} \sum_{k=1}^n [(h^k)^2 - (h^{k-1})^2] Q_{ij}^k = \sum_{k=1}^n Q_{ij}^k t^k z^k \\ D_{ij} &= \frac{1}{3} \sum_{k=1}^n [(h^k)^3 - (h^{k-1})^3] Q_{ij}^k = \sum_{k=1}^n Q_{ij}^k \left[ t^k (z^k)^2 + \frac{(t^k)^3}{12} \right] \\ F_{ij} &= \sum_{k=1}^n [h^k - h^{k-1}] C_{ij}^k = \sum_{k=1}^n C_{ij}^k t^k \end{aligned} \quad (2)$$

The corrugated cardboard is more complex than a laminated plate because of the fluting cores and the cavities between the three liners. Consequently some global effective stiffnesses in the matrix (1) obtained by the theory of laminated plates should be modified [5, 8, 10].

Considering a double corrugated cardboard and using  $a$ ,  $b$ ,  $c$ ,  $d$ , and  $e$  to represent the lower liner, the lower flute, the intermediate liner, the upper flute and the upper liner respectively (Fig. 2). The geometry of each flute is defined by the following equations:

$$\begin{cases} H^b(x) = \frac{h^b - t^b}{2} \sin\left(\frac{2\pi}{P^b} x\right) \\ \theta^b(x) = \tan^{-1}\left(\frac{dH^b(x)}{dx}\right) \end{cases} ; \begin{cases} H^d(x) = \frac{h^d - t^d}{2} \sin\left(\frac{2\pi}{P^d} x\right) \\ \theta^d(x) = \tan^{-1}\left(\frac{dH^d(x)}{dx}\right) \end{cases} \quad (3)$$

To homogenize a corrugated double wall panel, we consider a representative volume element (RVE). This volume must be sufficiently small relative to the dimensions of the entire panel. According to the

periodicity of the groove, we take a sinusoidal period of the groove as the characteristic length of the RVE. We calculate the mean or homogenized mechanical properties of the RVE and use them to model the 3D structure by the homogenized 2D plate. The idea is to cut the RVE into small vertical slices (thickness  $dx$ ) and to perform the integration according to the thickness (or the sum of the contributions of the 5 layers) on each slice. It can be seen that the piece of groove in the slice  $dx$  is inclined and that the mechanical properties of the groove obtained experimentally are valid only in its inclined plane, so it is better to work in the inclined local coordinates. Once the overall stiffnesses of each slice are obtained by integrating the thickness, homogenization along  $x$  is performed to calculate the average stiffness of all tranches over a period:

$$[A] = \frac{1}{P} \int_0^P [A(x)] dx ; [B] = \frac{1}{P} \int_0^P [B(x)] dx ; [D] = \frac{1}{P} \int_0^P [D(x)] dx ; [F] = \frac{1}{P} \int_0^P [F(x)] dx \quad (4)$$

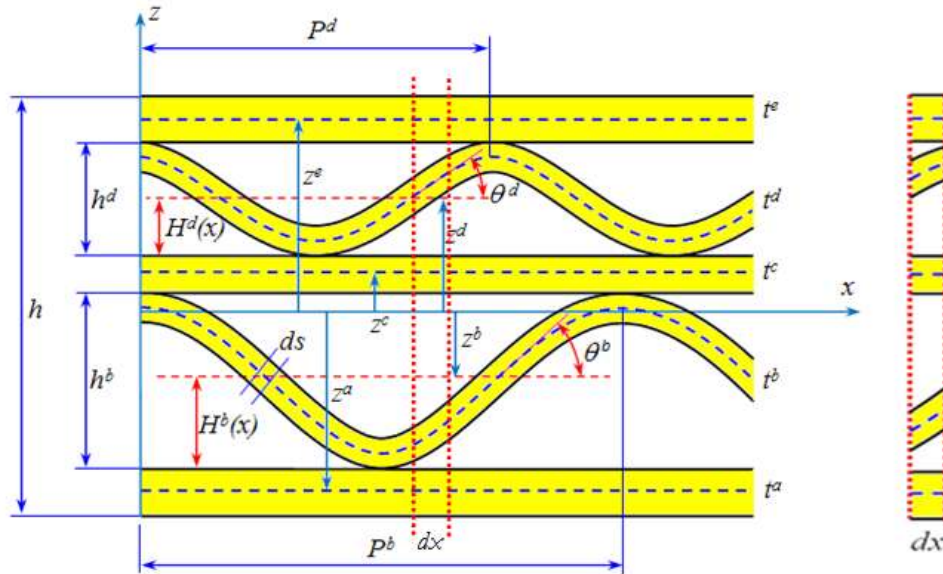


Fig. 2 Geometry of a double corrugated cardboard

### 2.1 Traction and bending stiffnesses

Since the vertical position ( $z$ ) of a groove portion ( $ds$ ) is a function of  $x$  and a thickness over its vertical section is a function of the angle of inclination of the groove  $\theta_x$  (Fig. 2), the equation (2) becomes [10]:

$$\begin{aligned} A_{ij} &= Q_{ij}^a t^a + Q_{ij}^b \frac{t^b}{\cos \theta^b} + Q_{ij}^c t^c + Q_{ij}^d \frac{t^d}{\cos \theta^d} + Q_{ij}^e t^e \\ B_{ij} &= Q_{ij}^a t^a z^a + Q_{ij}^b \frac{t^b}{\cos \theta^b} z^b + Q_{ij}^c t^c z^c + Q_{ij}^d \frac{t^d}{\cos \theta^d} z^d + Q_{ij}^e t^e z^e \\ D_{ij} &= Q_{ij}^a \left[ t^a (z^a)^2 + \frac{1}{12} (t^a)^3 \right] + Q_{ij}^b \left[ \frac{t^b}{\cos \theta^b} (z^b)^2 + \frac{1}{12} \left( \frac{t^b}{\cos \theta^b} \right)^3 \right] + \\ &+ Q_{ij}^c \left[ t^c (z^c)^2 + \frac{1}{12} (t^c)^3 \right] + Q_{ij}^d \left[ \frac{t^d}{\cos \theta^d} (z^d)^2 + \frac{1}{12} \left( \frac{t^d}{\cos \theta^d} \right)^3 \right] + Q_{ij}^e \left[ t^e (z^e)^2 + \frac{1}{12} (t^e)^3 \right] \end{aligned} \quad (5)$$

with

$$\begin{aligned} h &= t^a + h^b + t^c + h^d + t^e \\ z^a &= -\frac{h}{2} + \frac{t^a}{2} ; \quad z^e = \frac{h}{2} - \frac{t^e}{2} ; \quad z^c = -\frac{h}{2} + t^a + h^b + \frac{t^c}{2} \end{aligned}$$

$$z^b(x) = -\frac{h}{2} + t^a + \frac{h^b}{2} + \frac{1}{2}(h^b - t^b) \sin\left(\frac{2\pi}{P^b} x\right); \quad \frac{dz^b}{dx} = \frac{\pi(h^b - t^b)}{P^b} \cos\left(\frac{2\pi}{P^b} x\right); \quad \theta^b(x) = \tan^{-1}\left(\frac{dz^b}{dx}\right)$$

$$z^d(x) = \frac{h}{2} - t^e - \frac{h^d}{2} + \frac{1}{2}(h^d - t^d) \sin\left(\frac{2\pi}{P^d} x\right); \quad \frac{dz^d}{dx} = \frac{\pi(h^d - t^d)}{P^d} \cos\left(\frac{2\pi}{P^d} x\right); \quad \theta^d(x) = \tan^{-1}\left(\frac{dz^d}{dx}\right)$$

### 2.2 In-plane shear stiffness

We consider a corrugated flute having a length of semi period  $P/2$  along  $x$  and a width  $b$  along  $y$ . A shear force  $N_{xy}$  (per unit width along  $y$ ) applied on the MD section implies a transverse displacement  $v$  in  $y$  direction. If we unfold the flute to a flat plate, the shear stress  $\tau_{xy}$  can be easily calculated [8]:

$$\tau_{xy} = \frac{N_{xy}}{t^f} = G_{xy}^f \gamma_{xy} = G_{xy}^f \frac{v}{l/2} \quad (6)$$

where  $G_{xy}^f$  is the shear modulus of the flute,  $t^f$  is its thickness and  $l$  is its curvilinear length defined by:

$$l^f = 4 \int_0^{P^f/4} ds = 4 \int_0^{P^f/4} \frac{1}{\cos \theta^f} dx \quad \text{with} \quad \begin{cases} H^f(x) = \frac{h^f - t^f}{2} \sin\left(\frac{2\pi}{P^f} x\right) \\ \theta^f(x) = \tan^{-1}\left(\frac{dH^f(x)}{dx}\right) \end{cases} \quad (7)$$

where  $h^f$  is the fluting height (see Fig. 2).

Thus we obtain the in-plane shear behavior of the flute:

$$N_{xy} = \frac{G_{xy}^f t^f P^f}{l^f} \gamma_{xy} \quad (8)$$

We can demonstrate that the average of shear force on the CD section is equal to the shear force on the MD section. In fact, according to the reciprocity theorem, the shear stress flow along the flute on CD is equal to that on MD ( $\tau_{yx} = \tau_{xy} = N_{xy} / t = \text{const.}$ ); the component along  $x$  of this flow gives the shear force  $N_{yx}$ :

$$N_{yx} = \frac{l}{0,5P^f} \int_0^{0,5P^f} \tau_{yx} t^f \cos \theta^f ds = \frac{l}{0,5P^f} \int_0^{0,5P^f} N_{xy} dx = N_{xy} \quad (9)$$

So the relationship  $N_{xy} = N_{yx}$  on MD and CD is proven and shear stiffness is unique even if the two sections are very different.

Finally, for a cardboard with double flutes, the shear stiffness in the plane of the cardboard is given by the sum of the rigidities of five layers:

$$A_{33} = G_{xy}^a t^a + \frac{G_{xy}^b t^b P^b}{l^b} + G_{xy}^c t^c + \frac{G_{xy}^d t^d P^d}{l^d} + G_{xy}^e t^e \quad (10)$$

where the indices of  $a, b, c, d, e$  represent five layers respectively.

### 2.3 Transverse shear stiffness on CD section

It is difficult to directly determine the rigidity of transverse shear on the CD section because of the coupling of bending and transverse shear. According to the reciprocity theorem, Nordstrand et al. [7] proposed to replace the transverse shear under the shear force  $T_y$  (along  $z$ ) by a shear on the thickness under a force along  $y$ . The shear stiffness on the total thickness for double corrugated cardboard is obtained as follows:

$$F_{22} = G_{zy}^* h \quad (11)$$

with

$$G_{zy}^* = \frac{h}{\frac{t^a}{G_{zy}^a} + \frac{h^b}{G_{zy}^{b*}} + \frac{t^c}{G_{zy}^c} + \frac{h^d}{G_{zy}^{d*}} + \frac{t^e}{G_{zy}^e} + \frac{\gamma(1-\gamma)(P^d)^2}{G_{xy}^c t^c}}; \quad (12)$$

$$G_{zy}^{b*} = G_{12}^b \frac{4t^b h^b}{P^b l^b} \quad ; \quad G_{zy}^{d*} = G_{12}^d \frac{4t^d h^d}{P^d l^d}$$

where  $h$  is the total height of the cardboard,  $\gamma$  is a coefficient taking into account the effect of in-plane shear in the middle flat layer  $t^c$ .

#### 2.4 Transverse shear stiffness on MD section

It is still difficult to directly determine the rigidity of transverse shear on the CD section. So the transverse shear under the shear force  $T_x$  on the MD section (along  $z$ ) is replaced by a shear on the thickness under a force along  $x$ . In fact, this shearing problem is not really a shearing problem of five layers; it is dominated by the local bending of three flat layers and especially by the local bending of the two flutes. Thus this shearing problem becomes a bending problem of the flutes and liners which was solved by using the curved beam theory [7]. Assuming a double corrugated cardboard is the superposition of two single corrugated cardboards, the transverse shear stiffness relative to  $T_x$  for a double corrugated cardboard is obtained as follows:

$$F_{11} = G_{zx}^* h = h^2 \left( \frac{h^b}{G_{zx}^{b*}} + \frac{h^d}{G_{zx}^{d*}} \right)^{-1} \quad (13)$$

where  $G_{zx}^{b*}$  and  $G_{zx}^{d*}$  are the apparent shear modulus for two single corrugated cardboards calculated by using the analytical formulas developed by Nordstrand et al. [7] and implemented into our homogenization model.

#### 2.5 Torsion stiffness on CD and MD sections

For the torsion stiffness, Abbès B. and Guo Y.Q. [6] have theoretically demonstrated that the torsion of an orthotropic plate could be decomposed into two beam torsion problems, thus the torsion stiffness of a corrugated cardboard has been obtained:

$$D_{xy} = \frac{1}{4} \left( \frac{GJ_{MD}}{B} + \frac{GJ_{CD}}{L} \right) \approx \frac{GJ_{CD}}{4L} \quad (14)$$

where  $GJ_{MD}$  and  $GJ_{CD}$  are the beam torsion stiffnesses on MD and CD sections respectively ( $GJ_{MD} \ll GJ_{CD}$  for corrugated cardboards),  $L$  is the length along  $x$  and  $B$  is the width along  $y$  (see Fig. 1).

It is relatively easy to calculate  $J_{CD}$  for a cardboard with a single flute by considering it as a thin-wall closed section in which the contribution of the flute in torsion is negligible [6]. For the double corrugated cardboard, two flutes and the middle flat layer play an important role [8].

We have done the exact calculations by using the Bredt theory on three types of CD section, but in general, it is not easy to automatically find all adjacent cells and their common border lengths with the considered cell [8]. From these results, we find that the relative flux distribution is constant and independent along the widths and three liners constitute a closed shear flux loop and two flutes constitute another one. Therefore, we propose to divide the corrugated cardboard into two parts. The first part is composed of three flat liners and two additional vertical walls, leading to two closed cells. The second part is composed of two flutes, leading to a single closed cell. Finally, the torsion rigidity of a homogeneous plate can be obtained as follows:

$$D_{33} \approx \frac{GJ_{CD}}{4L} = \frac{GJ_{liner}}{4L} + \frac{GJ_{flute}}{4P^b P^d} \quad (15)$$

$$= G \frac{t^a(t^c + t^e)S_1^2 + t^e(t^a + t^c)S_2^2 + 2t^a t^e S_1 S_2}{t^a + t^c + t^e} + G \frac{t^b t^d (P^d S_{bc} + P^b S_{cd})^2}{P^b P^d (P^d t^d l^b + P^b t^b l^d)}$$

where  $S_{bc}$  is the surface enveloped by the inferior flute and internal liner on a period  $P^b$ ;  $S_{cd}$  is the surface enveloped by the internal liner and superior flute on a period  $P^d$ ; and  $l^b, l^d$  are the curvilinear lengths of the two flutes on a period.

### III. HOMOGENEOUS SOLID WITH THREE LAYERS AND THREE MATERIALS

The homogenization model developed in the previous sections provides twelve global stiffnesses ( $A_{11}, A_{12}, A_{22}, A_{33}, B_{11}, B_{12}, B_{22}, B_{33}, D_{11}, D_{12}, D_{22}, D_{33}$ ) of the homogenized equivalent plate. However, this model does not simulate the crush of an interlayer between two bottles for example; this crush gives an impression that prevents sliding of bottles on the interlayer. Therefore, we propose to transform this plate into a solid composed of three layers (layers  $a, c, e$ ) consisting of three different materials in order to take into account not only the behavior of shell but also the behavior of compression through the thickness of the corrugated cardboard (Fig. 1). For this solid composed of three layers, the laminate theory is used and results in twelve equations with twelve unknowns:

$$\begin{aligned} A_{11} &= Q_{11}^a t^a + Q_{11}^c t^c + Q_{11}^e t^e & ; & & B_{11} &= Q_{11}^a t^a z^a + Q_{11}^c t^c z^c + Q_{11}^e t^e z^e \\ A_{12} &= Q_{12}^a t^a + Q_{12}^c t^c + Q_{12}^e t^e & ; & & B_{12} &= Q_{12}^a t^a z^a + Q_{12}^c t^c z^c + Q_{12}^e t^e z^e \\ A_{22} &= Q_{22}^a t^a + Q_{22}^c t^c + Q_{22}^e t^e & ; & & B_{22} &= Q_{22}^a t^a z^a + Q_{22}^c t^c z^c + Q_{22}^e t^e z^e \\ A_{33} &= Q_{33}^a t^a + Q_{33}^c t^c + Q_{33}^e t^e & ; & & B_{33} &= Q_{33}^a t^a z^a + Q_{33}^c t^c z^c + Q_{33}^e t^e z^e \end{aligned} \tag{16a}$$

$$\begin{aligned} D_{11} &= Q_{11}^a c^a + Q_{11}^c c^c + Q_{11}^e c^e & ; & & c^a &= \left[ t^a (z^a)^2 + \frac{1}{12} (t^a)^3 \right] \\ D_{12} &= Q_{12}^a c^a + Q_{12}^c c^c + Q_{12}^e c^e & ; & & c^c &= \left[ t^c (z^c)^2 + \frac{1}{12} (t^c)^3 \right] \\ D_{22} &= Q_{22}^a c^a + Q_{22}^c c^c + Q_{22}^e c^e & ; & & c^e &= \left[ t^e (z^e)^2 + \frac{1}{12} (t^e)^3 \right] \\ D_{33} &= Q_{33}^a c^a + Q_{33}^c c^c + Q_{33}^e c^e & ; & & & \end{aligned} \tag{16b}$$

where  $A_{11}, \dots, D_{33}$  are the global rigidities of the homogenized plate obtained by our homogenization model (H-2D-model),  $t^a, t^c, t^e$  are the thicknesses of the three layers imposed by the user;  $Q_{11}^a, \dots, Q_{33}^e$  are the twelve unknowns needed to find.

We can rewrite the twelve equations above in the following matrix form:

$$\begin{Bmatrix} Q_{ij}^a \\ Q_{ij}^c \\ Q_{ij}^e \end{Bmatrix} = \begin{bmatrix} t^a & t^c & t^e \\ e^a z^a & e^c z^c & e^e z^e \\ c^a & c^c & c^e \end{bmatrix}^{-1} \begin{Bmatrix} A_{ij} \\ B_{ij} \\ D_{ij} \end{Bmatrix} \quad \text{with } ij = 11, 22, 33, 12 \tag{17}$$

The resolution of these four systems of equations allows us to obtain the twelve unknowns. For each layer ( $a, c$  and  $e$ ), we can calculate the parameters of three materials as follows:

$$\{\sigma\} = \begin{Bmatrix} \sigma_x \\ \sigma_y \\ \sigma_{xy} \end{Bmatrix} = \begin{bmatrix} Q_{11} & Q_{12} & 0 \\ Q_{21} & Q_{22} & 0 \\ 0 & 0 & Q_{33} \end{bmatrix} \begin{Bmatrix} \varepsilon_x \\ \varepsilon_y \\ \gamma_{xy} \end{Bmatrix} = \begin{bmatrix} \frac{E_x}{1-\nu_{xy}\nu_{yx}} & \frac{\nu_{xy}E_y}{1-\nu_{xy}\nu_{yx}} & 0 \\ \frac{\nu_{yx}E_x}{1-\nu_{xy}\nu_{yx}} & \frac{E_y}{1-\nu_{xy}\nu_{yx}} & 0 \\ 0 & 0 & G_{xy} \end{bmatrix} \begin{Bmatrix} \varepsilon_x \\ \varepsilon_y \\ \gamma_{xy} \end{Bmatrix} \tag{18}$$

$$\begin{aligned} \nu_{xy} &= \frac{Q_{12}}{Q_{22}} & ; & & \nu_{yx} &= \frac{Q_{12}}{Q_{11}} & ; & & E_x &= Q_{11}(1-\nu_{xy}\nu_{yx}) & ; & & E_y &= Q_{22}(1-\nu_{xy}\nu_{yx}) \\ G_{xy} &= Q_{33} & ; & & G_{xz} &= \frac{F_{11}}{h} & ; & & G_{yz} &= \frac{F_{22}}{h} \end{aligned} \tag{19}$$

To take into account the crushing of the flutes in the thickness of corrugated cardboard, the material is assumed elasto-plastic in the  $z$  direction in which only the constraint intervenes such that:



Yield criterion:  $f = |\sigma_z| - \bar{\sigma}$  (20)

Hardening law:  $\bar{\sigma} = E_0 (\epsilon_0 + \bar{\epsilon}_p)^n$  (21)

where  $E_0, \epsilon_0, n$  are the parameters of the elasto-plastic behavior used. The model thus described has been implemented in software Abaqus/Explicit with a user program VUMAT.

#### IV. RESULTS AND DISCUSSION

To validate our homogenized model (H-3D-model), we carried out the experiment and numerical simulation of crushing and bending of corrugated cardboard plate placed between the mortar and pestle system assumed rigid with Abaqus (Fig. 3). The diameter of the plate, pestle, and mortar are 168 mm, 34 mm, and 60 mm respectively. The coefficient of friction between plate and mortar-pestle system is assumed 0.1.

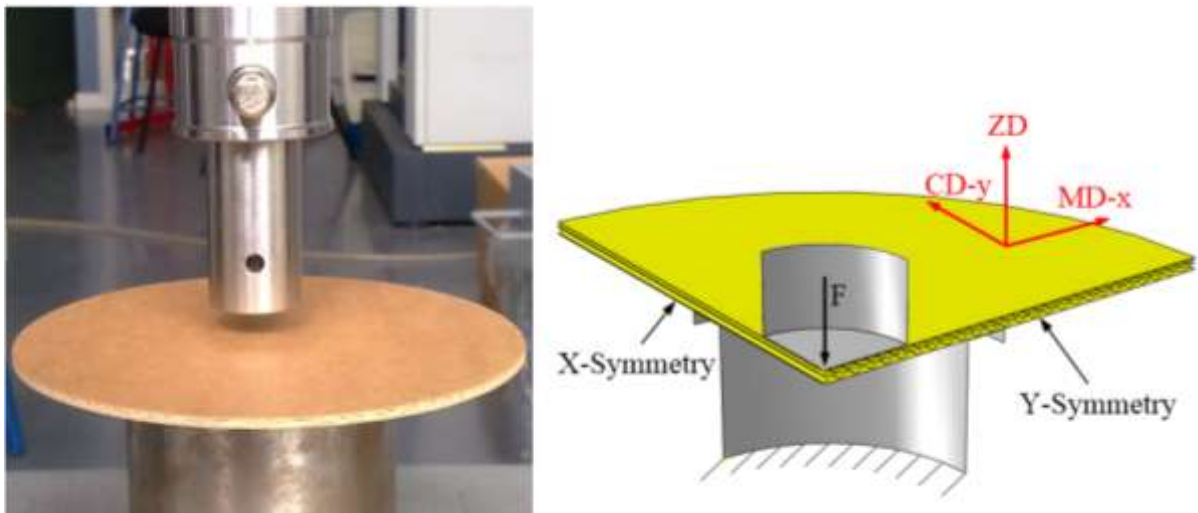


Fig. 3 Crushing and bending test and boundary conditions of the cardboard plate

We fix the mortar and apply a vertical force on the pestle. As corrugated cardboard plate is symmetrical, it is better to simulate a quarter of the plate to save computing time, the boundary conditions are X-symmetry and Y-symmetry on two sides of a quarter of the plate. The dimensions of the cardboard are given in Fig. 4 and the properties of all papers of the cardboard are given in Table 1.

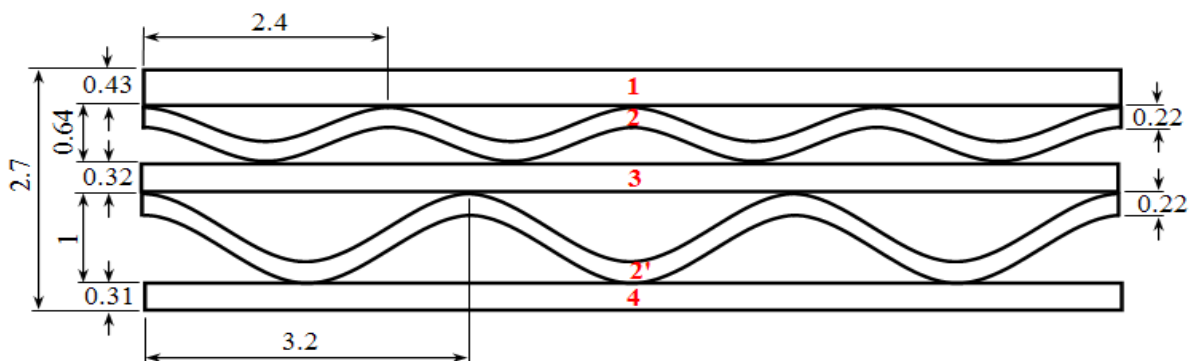


Fig. 4 Geometry of CD section for the double corrugated cardboard

The elastic properties of the solid equivalent determined by using equations (17), (18), and (19) are given in Table 2. To obtain the law of elasto-plastic through the thickness of the cardboard using equations (20) and (21), we simulate the crushing of a cardboard with Abaqus 3D shell elements. The results are also given in Table 2.

Table 1 Properties of papers forming corrugated cardboard

	$E_1(\text{MPa})$	$E_2(\text{MPa})$	$\nu_{12}$	$G_{12}(\text{MPa})$
<b>Paper 1</b>	2483.3	1322.7	0.3485	488.3
<b>Paper 2,2'</b>	720.8	739.8	0.4387	274.8
<b>Paper 3</b>	1887.4	693.1	0.4777	535.5
<b>Paper 4</b>	2124.5	1027.0	0.2176	622.8

Table 2 Properties of equivalent solid

	<b>Layer a</b>	<b>Layer c</b>	<b>Layer e</b>
<b>Thickness (mm)</b>	1.7	1.6	1.7
$E_1(\text{MPa})$	106.3078	1058.9133	287.4231
$E_2(\text{MPa})$	55.1555	685.303	162.1973
$E_3(\text{MPa})$	17.365	17.365	17.365
$\nu_{12}$	0.0251	0.2542	0.3544
$G_{12}(\text{MPa})$	37.0374	336.2898	48.891
$G_{13}(\text{MPa})$	9.4	9.4	9.4
$G_{23}(\text{MPa})$	12.637	12.637	12.637
$E_0(\text{MPa})$	0.7791	0.7791	0.7791
$n$	0.0037	0.0037	0.0037
$\epsilon_0$	0.0292	0.0292	0.0292

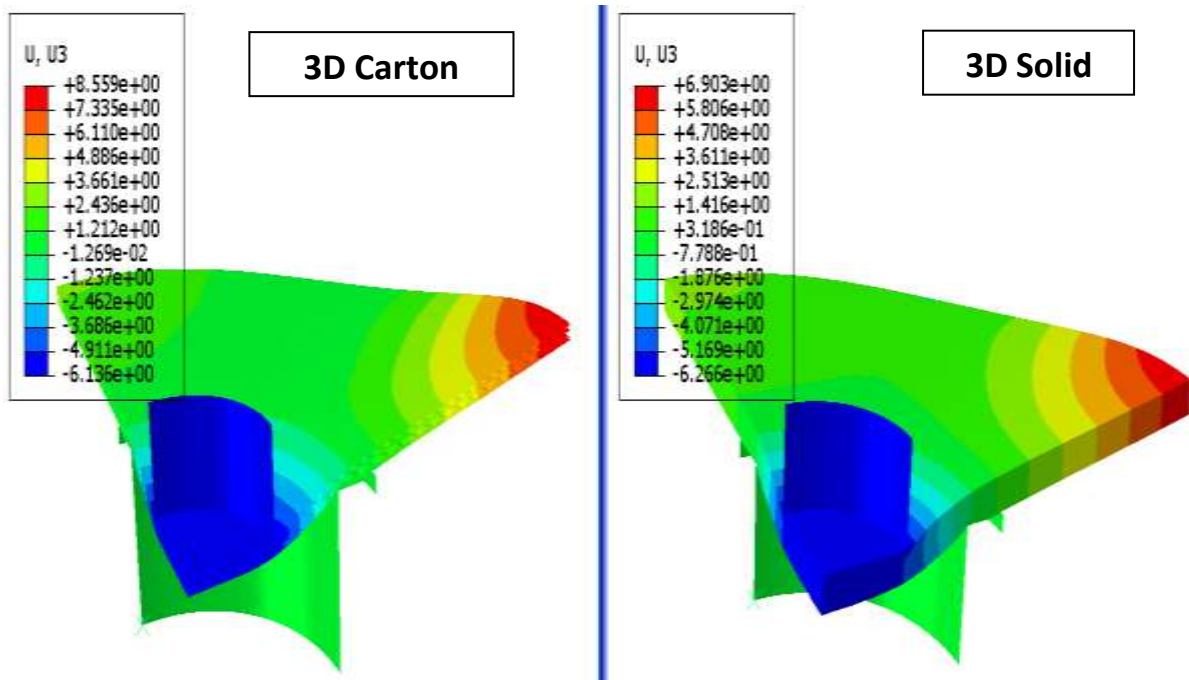
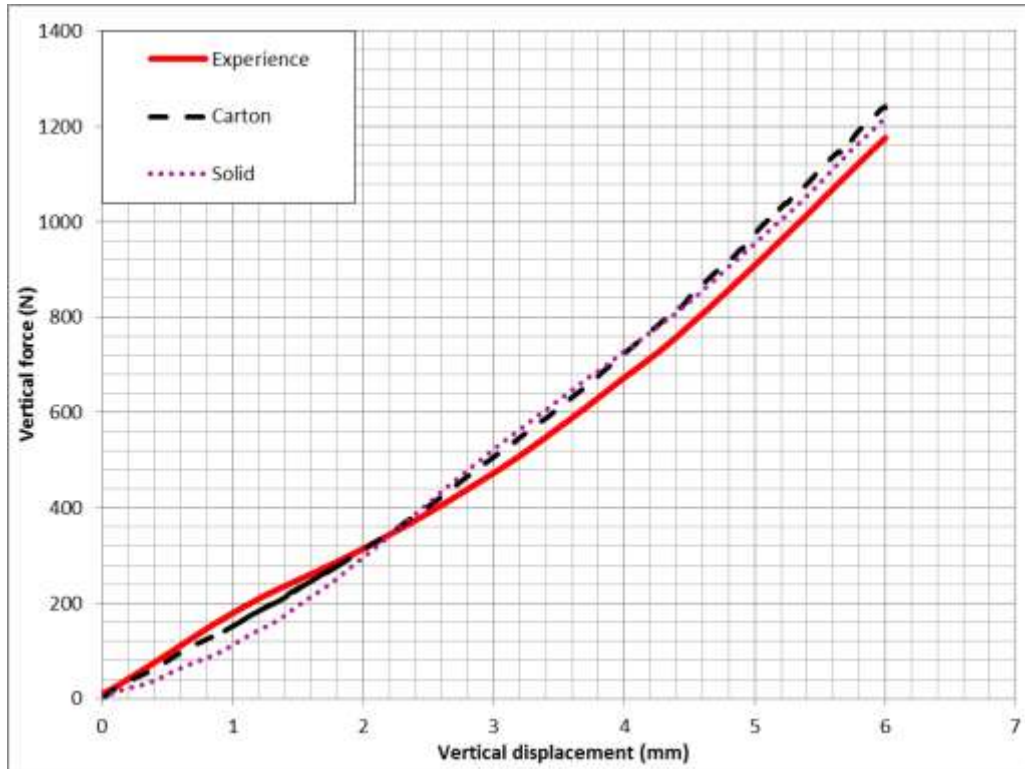


Fig. 5 Iso-values of displacement for the double corrugated cardboard





**Fig. 6** Crushing and bending of cardboard

For the Abaqus 3D simulation, the corrugated cardboard is discretized into 50894 S4R shell elements, 52286 nodes. For the 3D solid simulation using Abaqus through the user subroutine VUMAT, the solid is discretized into 10098 C3D8 hexahedral elements and 15831 nodes.

The deformed shapes together with the iso-values of displacement of the panel after loading obtained by 3D shell Abaqus and our 3D solid model simulations are shown in Fig. 5. We observe that the Abaqus 3D simulation is very time consuming using 9926 s CPU time, but our 3D solid homogenization model simulation is very fast, using only 328 s (30 times faster). Fig. 6 shows the experimental and numerical curves of force–displacement for the double corrugated cardboard. We note that the 3D shell Abaqus and 3D solid model simulations give very close crushing and bending behaviors and give the results very close with the experimental results. The comparison demonstrates that the proposed 3D solid analytic homogenization model for the double corrugated core sandwich plates is quite accurate and efficient, and it can be used to simulate large-scale complex packaging systems and structures.

## V. CONCLUSIONS

In this article, a 3D complete analytical homogenization model for the orthotropic composite plates with the type of double corrugated cardboard has been developed allowing simulating the non-linear behavior through the thickness of corrugated cardboard without modeling the 3D flutes. This model has been implemented in Abaqus/Explicit through the user subroutine VUMAT. Our 3D solid model was validated by experimental tests and simulations on the crushing and bending of cardboard with double corrugated core and showed that it was more effective than the 3D shell model in Abaqus. The FE simulation results of two models agree well with the experimental results.

## REFERENCES

- [1] Carlsson, L. A., Nordstrand, T. and Westerlind, B., On the elastic stiffness of corrugated core sandwich plate, *Journal of Sandwich Structures and Materials*, 3, 2011, 253–267.
- [2] Aboura, Z., Talbi, N., Allaoui S. and Benzeggagh, M. L., Elastic behaviour of corrugated cardboard: experiments and modeling, *Composite Structures*, 63, 2004, 53–62.
- [3] Buannic, N., Cartraud, P. and Quesnel, T., Homogenization of corrugated core sandwich panels, *Composite Structures*, 59, 2003, 299–312.
- [4] Biancolini, M. E., Evaluation of equivalent stiffness properties of corrugated board, *Composite Structures*, 69, 2005, 322–328.

- [5] Talbi, N., Batti, A., Ayad, R. and Guo, Y. Q., An analytical homogenization model for finite element modelling of corrugated cardboard, *Composite Structures*, 69, 2005, 322–328.
- [6] Abbès, B. and Guo, Y. Q., Analytic homogenization for torsion of orthotropic sandwich plates: application to corrugated cardboard, *Composite Structures*, 92, 2010, 699–706.
- [7] Nordstrand, T., Carlsson, L. A. and Allen, H. G., Transverse shear stiffness of structural core sandwich, *Composites Structures*, 27, 1994, 317-329.
- [8] Duong, P. T. M. et al, An analytic homogenization model for shear-torsion coupling problems of double corrugated-core sandwich plates, *Journal of Composite Materials*, 47, 2013, 1327-1341.
- [9] Hammou, A. D., Duong, P. T. M., Abbès, B., Makhoulf, M. and Guo, Y. Q., Finite-element simulation with a homogenization model and experimental study of free drop tests of corrugated cardboard packaging, *Mechanics & Industry*, 13, 2012, 175-184.
- [10] Duong, P. T. M., and Ngo, N. K., An analytic homogenization model in traction and bending for orthotropic composite plates with the type of double corrugated cardboard, *Vietnam Journal of Mechanics*, 38, 2016, 205-213.
- [11] Biancolini, M. E. and Brutti, C., Numerical and Experimental Investigation of the Strength of Corrugated Board Packages, *Packaging Technology and Science*, 16, 2003, 47–60.
- [12] Rami, H. A., Choi, J., Wei, B. S., Popil, R. and Schaepe, M., Refined Nonlinear Finite Element Models for Corrugated Fiberboards, *Composite Structures*, 87, 2009, 321–333.